Inspection of production alternating PSM reticles using UV-based 365 nm reticle inspection tool

Anja Rosenbusch, Michael Har-zvi,[*] Gidi Gottlib,*

[*]Etec Systems, Inc., an Applied Materials company,
Oppenheimer St. 9, Park Tower, Rehovot 76705 Israel

Etec Systems, Inc., an Applied Materials company,
26460 Corporate Avenue, Hayward, CA 94545 USA

Keywords: Phase shift mask, 193 nm AAPSM, 248 nm AAPSM, *i*-line inspection, mask inspection, reticle enhancement technique (RET)

1 ABSTRACT

The paper presents results of a thorough study using the UV-based die-to-database mask inspection system ARIS[TM]100i for the inspection of alternating phase shifting masks (AAPSM) designed for ArF (193nm) technology. Specially designed test masks were used to investigate sensitivity limitations of the i-line tool. Main focus is on phase errors, which were treated as a function of defect size, phase, and mask location. In addition, production reticles were inspected using a specially developed sensitivity AAPSM. Production issues like false defect rate and data preparation were addressed. The paper is concluded with a short printability analysis of different phase defects detected during the experiment.

2 INTRODUCTION

As the cost of lithography equipment within the fabs continues to rise, while the requirements for feature size continue to shrink, fabs are debating the most cost-effective solutions. One possibility is to use advanced and proven reticle enhancement technologies (RET) such as attenuated, alternating phase shift masks (AAPSM); another is to install advanced 193 nm lithography equipment and to “buy” additional resolution. Both solutions carry a high price tag, because AAPSM reticles are still relatively expensive. One of the contributors to the high cost of AAPSM reticles comes from the challenge of inspecting them.

This paper focuses on the inspection of alternating PSMs designed for the 248nm and 193nm lithography generation. As DUV (deep ultraviolet) based inspection tools are not yet available, *i*-line based inspection must be used to inspect this generation of masks. The performance of a reticle inspection system is limited by the wavelength of the light source used. This limitation gets especially important when inspecting PSMs. The main characteristic of an alternating PSM is that it contains areas of glass with different thicknesses, which influence the amount of transmitted light. The challenge for the reticle inspection tool is to identify defects consistently through varying glass thicknesses. The gap between the inspection wavelength (365nm) and the stepper wavelength (248nm) may cause problems, because the transmission level of 248nm translates into a higher transmission on the inspection tool using 365nm illumination.

The study described in this paper uses Etec’s ARIS100*i* die-to-database inspection tool to inspect AAPSMs for the 248nm and 193nm generation. Production poly gate levels designed for ArF lithography are inspected. Inspection sensitivity and quality with regard to different defect types are evaluated. A defect sensitivity specification for 248nm defect inspection using *i*-line illumination is proposed. False defect rates and calibration issues are investigated for different types of production masks. Defect printability and its importance for mask qualification and mask shop cycle time are addressed briefly.

3 EXPERIMENTAL SETUP

This section describes issues that came up when attempting the inspection of production AAPSMs. Before the inspection experiment was started, the specially developed sensitivity AAPSM was compared with binary performance results using A09 sensitivity. Next, data preparation issues due to the structure of different AAPSM designs needed to be resolved.

3.1 Test mask description

The study was based on the inspection of three different masks. Due to confidentiality issues, no details about the mask processes used can be provided:

- Mask 1 AAPSM test design targeted for the 130nm generation using 248nm lithography. The 0°/180° AAPSM SRAM test mask contains 60°, 120°, and 180° plated phase errors.
- Mask 2 A poly gate layer designed for 130nm technology node. The intended wavelength is 193nm. The mask inspection was done in a production environment.
- Mask 3 A production metal layer designed for 193 nm technologies.

3.2 Sensitivity comparison between AAPSM and binary inspection setup

The inspection system ARIS100i offers a special PSM application. In this work the A09 magnification using a 0.17µm pixel size and the AAPSM sensitivity were used. This magnification was chosen, because it is standard production sensitivity for 130nm-generation masks, providing a throughput of approximately two hours per plate. The sensitivity was evaluated using the Verithoro VT690. Figure 1 displays the sensitivity comparison. The rows contain the different VT defect types. The columns represent different defect sizes. The inspection was repeated 10 times. Green indicates detection with 100% capture rate (detected in all runs). Dark gray indicates detection with a below 100% capture rate. Light gray stands for non-detection. The red line represents the A09 sensitivity specification of the ARIS100i system. It can be observed that the AAPSM sensitivity is very similar to the standard A09. Only for two VT types (truncation defects I and K), the A09 is slightly better.

Figure 1: Comparison of AAPSM and standard A09 inspection sensitivity using the VT690 mask. The red line represents the standard ARIS100i sensitivity for binary masks (100% capture rate). The PSM sensitivity is very compatible for almost all defect types. Only for truncation defects (VT types I and K) the A09 is slightly better than the AAPSM.

3.3 Specific data preparation for AAPSM masks

Another issue needing attention was the data preparation for the die-to-database inspection. The basic idea of an alternating phase shift masks is to enhance image quality during stepper exposure. This is done by alternating the phase of features on the mask, which is achieved by etching the areas differently. The phase difference between the areas is usually 180°. Each PSM works on this principle. However, the implementation may differ from user to user. Figures 2a and 2b present two implementation examples. Both masks offer a phase shift of 180°. The mask shown in Figure 2a presents the classical PSM implementation. The mask consists of non-etched and etched spaces. The phase difference is 180°. Figure 2b shows a more advanced AAPSM implementation. Both phases are etched, maintaining the phase difference of 180°. In addition, a chrome undercut is performed to enhance image quality (reduce intensity imbalance).

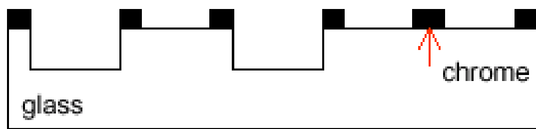

Figure 2a: Typical design layout of AAPSM. The mask contains un-etched and etched areas. The etched Cr areas define the 180° phase shift.

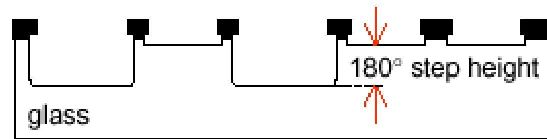

Figure 2b: More challenging design layout of AAPSM. The mask contains areas having two different etch levels. The difference in etch depth defines the 180° phase shift. In addition, a Cr underetch bias applied to enhance image quality of this mask.

AAPSM masks are manufactured using several mask writing steps. To inspect masks similar to the one in Figure 2b, additional data preparation needs to be done. The reason can be observed in Figure 3. Due to a different underetch amount of 0° and 180° phases, the linewidth is different for the two phases. The inspection database has to be adjusted accordingly. The databases of all writing steps are needed. The PSM design has to be known or analyzed, mask features have to be biased accordingly to the different phases, and the inspection setup has to be adapted. To accomplish this sophisticated data manipulation, a special AAPSM application was designed.

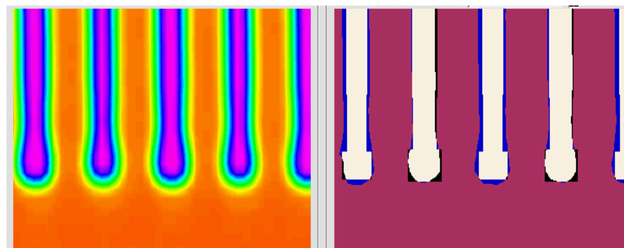

Figure 3: Mask image captured during inspection (left) and overlaid with database (right). The line width of every second line is different due to selected AAPSM design. Die-to-database inspection needs to cope with that.

4 MASK INSPECTION RESULTS

In this section the mask inspection results for the three different masks are provided. The work performed on the test mask was focused on understanding detection limitations of an i-line inspection system. Eighteen different types of phase errors, three different phases and six different defect locations, were monitored. In addition, the work on 30° phase errors was started, but has not been finished yet. The work on the production masks was focused on proving

production-worthiness of the AAPSM application of the ARIS system. Runability questions like data preparation and false defect rate were checked. In addition, printability was verified on some of the investigated defects.

4.1 AAPSM test masks

Before investigating the inspection of production reticles, test masks were used to define inspection limitations of the ARIS100i system used. Specially designed 248nm test masks containing programmed phase defects were used. The first mask contained defects of four different phases/material: Chrome defects, and 60°, 120°, 180° phase defects. Defects on six different locations were investigated: 180° stand for deep shifter, 0° stands for shallow shifter area.

- (D1) Dots/bumps in 180°-shifter centers
- (D2) Dots/pit in 0°-shifter centers
- (D3) Protrusion/bump in upper corner of 180°-shifter
- (D4) Protrusion/pit in upper corner of 0°-shifter
- (D5) Protrusion/bump on mid-gate edge of 180°-shifter
- (D6) Protrusion/pit on mid-gate edge of 0°-shifter

Figure 4 summarizes the sensitivity results. The programmed defect size is displayed at the top of each column. Gray indicates that the defect was not resolved during mask writing. Green means, that the ARIS system could see the defect. The numbers in the table are the measured defect sizes of the largest defect not seen and the smallest defect size found by the ARIS100i.

size (nm)	80	120	160	200	240	280	320	400	480	560	size (nm)	80	120	160	200	240	280	320	400	480	560
Cr D1						19	124				120 D1					43	57				
Cr D2					24	127					120 D2		173	221							
Cr D3					262	284					120 D3									328	412
Cr D4				223	255						120 D4						113	168			
Cr D5			141	181							120 D5								228	298	
Cr D6			152	170							120 D6			220							
180 D1					36	80					60 D1							113			
180 D2		244									60 D2			179	305						
180 D3								224	302		60 D3									342	423
180 D4					278	341					60 D4							317	380		
180 D5								208	281		60 D5								236	321	
180 D6		238									60 D6			170	305						

Figure 4: Defect sensitivity chart. The experiment was performed to define inspection limitations using a production setup. Green indicates that the defect could be seen by the ARIS100i system.

When comparing sensitivity for defects in the center, edge, and corner of the shifter areas, a clear advantage for center defects can be observed. Although i-line optics is used for the inspection, the optics actually recognizes a freestanding defect very well. The closer the defect is located to the main feature the more difficulties the tool seems to have. Next, bump and pit defects were compared. In the case of chrome and 180° defects, bumps were better identified than pits. For the smaller phase errors, a real conclusion could not be made, as the actual defect sizes were quite different for bump and pit defects.

Figure 5 displays an example of a planted mid-gate defect on the first test mask as recorded by the ARIS100i system. The question that remains is whether this defect is severe. Or in other words, is it necessary to repair this defect or can it be left as is. The importance of this question gets clearer if assessing the risk attached to a PSM repair. What if the repair damages the mask? What if the defect is not repairable? Figures 6 and 7 display the results of an AIMS study of two defect types. Numerical aperture and coherence were chosen to match the mask user's lithography settings.

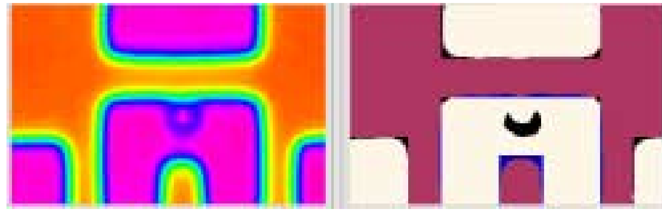

Figure 5: Example image of 0.32µm 120° phase error as seen by inspection system (left) and overlaid with database (right).

Figure 6 displays the sensitivity chart for defect D1, a defect in the center of the shifter area. Green indicates that the defect was identified as printable using the MSM100 system. Yellow indicates that the defect could be seen by the ARIS system. It can be seen that, for this defect, the tool is actually more sensitive than necessary. It identifies defects too small to have any impact on aerial image during stepper exposure.

CR	Dot in deep shifter center	0	0	0	0	0	19	124	248	378	482
180º	Bump in deep shifter center	0	0	0	26	36	80	121	175	256	347
120º	Bump in deep shifter center	0	0	0	22	43	57	83	177	274	351
60º	Bump in deep shifter center	0	0	0	0	42	61	113	191	286	361

Figure 6: Sensitivity chart for defect type D1. Green indicates that the inspection system could find the defect and that the defect is identified as printable using the MSM100 system. Yellow stands for detection of a not printable defect.

Defect D5 is a protrusion or pit on the mid-gate edge of the 0°-shifter. The proximity to the main feature is very close. In this example, two different issues can be observed. For the 60°-phase cases, the ARIS100i system finds all printable defects, plus an additional case, where the defect is too small to have an impact on aerial image intensity. In the case of 120° and 180° phase error, the ARIS100i system actually cannot see defect sizes, which have printable impact on the aerial image of this mask. In other words, the tool misses a defect, which may impact the wafer exposure result. As the planted defects are close to the main features finding and repairing this defect may be critical.

In addition to illustrating that i-line tools may not see all phase defects in a given mask, the example also points to another issue worth discussion. Figure 4 displays the state-of-the-art way to characterize inspection sensitivity: qualifying an inspection tool by asking for a sensitivity chart. However, Figure 7 shows an example, where the information obtained using this standard procedure does not guarantee a functional mask. Defects are missed. New inspection methodologies and defect specification are needed to overcome this problem.

CR	Protrusion in deep shifter on mid-gate edge	65	119	141	181	211	255	300	*	*	*
180º	Bump in deep shifter on mid-gate edge	0	0	0	57	73	91	125	208	281	363
120º	Bump in deep shifter on mid-gate edge	0	0	0	52	61	122	148	228	298	386
60º	Bump in deep shifter on mid-gate edge	0	0	0	40	75	110	159	236	321	407

Figure 7: Sensitivity chart for defect type D5. Green indicates that the inspection system could find the defect and that the defect is identified as printable using the MSM100 system. Yellow stands for detection of a not printable

defect. Red identifies defects that could not be seen using the ARIS100i optics, but were classified as printable using the MSM100.

4.2 Production Poly Layer

In the previous section, the detection sensitivity of the ARIS100i tool was investigated for AAPSMs. After base-lining the tool limitations, the ARIS100i system was used for 193nm production AAPSM reticles. The inspection was done with the AAPSM application using a 0.17µm pixel size. As an advanced AAPSM design was used, data preparation as described earlier was done. The quantitative results are:

- Inspection time	Below two hours
- Number of defects found	335
- Chrome extensions	21
- Chrome intrusions	7
- Line end shortening (LES)	84
- Inverse LES	68
- False defect rate	52

The inspection run found 335 defects with a false defect rate of 52. The main defect types found were extensions and intrusions as well as line end shortening. After defect review seven defects were defined to be critical and were sent for repair and review.

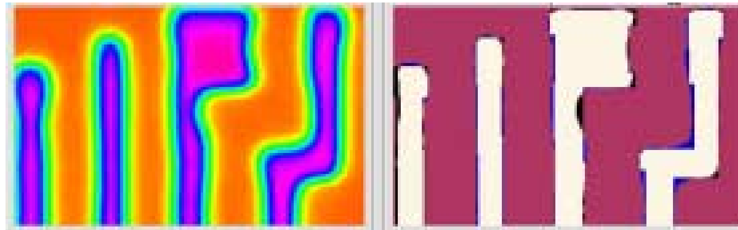

Figure 8: Example of defect found during die-to-database inspection. The left image shows the chrome extension defect as it is seen by the ARIS system. The right side shows the overlay of the binarized inspection image and database.

Figures 8 and 9 present some defect examples of the inspected mask. In Figure 8, a chrome extension defect is displayed. The left image is taken from the inspection system. The right picture shows the overlay of binarized inspection image and database. The chrome extension can be seen clearly in both pictures. Figure 9 displays AIMS images incorporating the user's lithography settings. All three defects displayed have a severe impact on the aerial image of the mask.

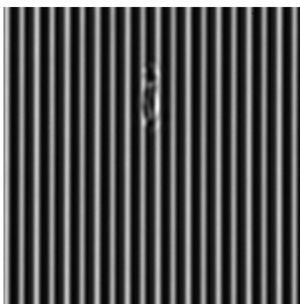

Figure 9a: Aerial image of chrome extension defect.

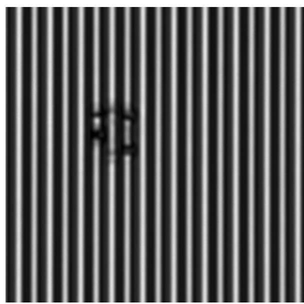

Figure 9b: Aerial image of inverse LES defect.

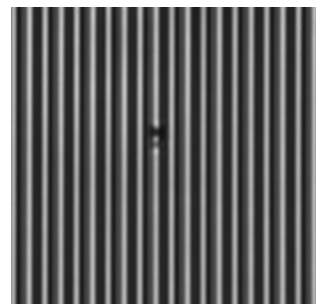

Figure 9c: Aerial image of chrome intrusion defect.

4.3 Production Metal Layer

The forth mask inspected using AAPSM sensitivity is a metal layer designed for the 130nm technology generation. The inspection finished without any issues. The false defect rate was in the same range as binary masks of the same complexity. Figure 10 shows a couple of examples of defects found during this inspection.

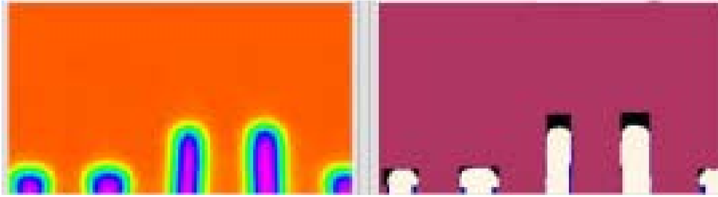

Figure 10a: Inspection image of LES effect (left) and overlay with database (right). The line-end shortening can be clearly seen on the right side.

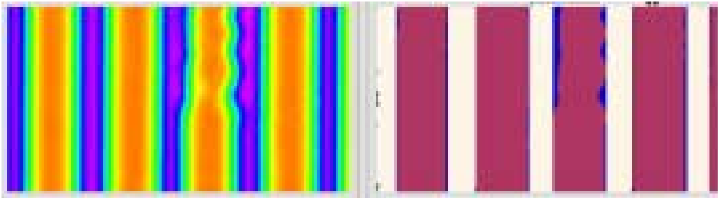

Figure 10b: Inspection image of edge roughness defect (left) and overlay with database (right)..

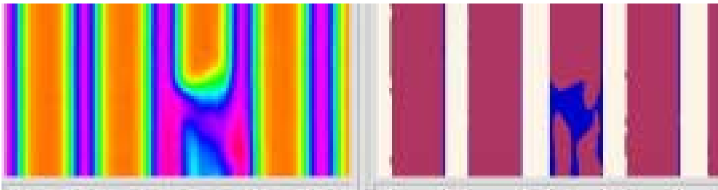

Figure 10c: Inspection image of missing chrome defect (left) and overlay with database (right). The reason of this defect could be a defective mask blank.

4.4 Printability impact analysis

As discussed earlier in this paper, defect size and type are not sufficient to decide whether a defect is severe and needs repair or not. In the above-presented cases, the ARIS100i system identified defects that do not impact aerial image. In the production examples, more than 50% of the found defects had no impact on the aerial image of the mask. The solution to this problem requires additional defect analysis, usually done manually or software-supported., which is then followed by repair and defect review (using for example the AIMS microscope).

As a practical example of the issue, let us assume that defect classification, repair, and AIMS verification takes 30 minutes per defect. If 5 defects are repaired and reviewed, 150 minutes are added to the mask cycle time. In the case of 10 additional defects, the time increases to 300 minutes. Additionally, there is a certain risk of damage to the mask during repair and of missing a critical defect due to repair/review limitations.

At the same time, the inspection may miss critical defects due to inspection tool limitations as described earlier.

5 CONCLUSIONS

The paper presents a practical approach of UV-based mask inspection for today's AAPSM applications. Sensitivity and productivity of the die-to-database system ARIS100i were investigated. The AAPSM sensitivity is similar to the sensitivity for binary masks. For phase errors, the isolated cases were detected very easily. The closer a defect is to the main feature, the more challenging the inspection gets. The same trend could be observed for the phase of a defect. The smaller the phase error is, the less conclusive the results were. Test runs under production environment proved that throughput and false defect rate were the same as for binary plates. The throughput using the AAPSM sensitivity was well below two hours.

However, high-resolution inspection seems not to be comprehensive enough to inspect advanced mask plates. Two issues were identified. The tools usually overdetect defects. When adding printability to the defect classification, many small defects can be omitted, as they do not impact the aerial image of a mask. In a time when mask shops are trying to automate mask manufacturing and yield improvement, while mask costs and cycle time are becoming a very critical issue, overdetection of the mask inspection system may severely impact productivity.

An even more severe problem is that even high-resolution i-line systems may not be comprehensive enough for next-generation mask inspection needs. As shown in this paper, certain defect types may not be detected. In other words, a maskmaker cannot guarantee a defect-free AAPSM because inspection cannot guarantee a 100% capture rate for all defect types. Work has to be done to overcome this problem by introducing new mask defect specifications and mask inspection methodologies.

6 REFERENCES

1. K. Phan, C. Spence, S. Dakshina-Murthy, V. Bala, A. Williams, S. Strener, R. Eandi, J. Li, L. Karklin, "Comparison of Binary Mask Defect Printability Analysis Using Virtual Stepper System and Aerial Image Measurement System, *Proc.SPIE* vol. 3873, pp. 681-692, (1999).
2. E. Poortinga, J. Novak, B. Eynon, "A Comparison of Software and Physical Simulation Tools on an Embedded-Attenuated Phase Shift Mask", Micro Magazine Vol. 18 #6, pp. 69-91 (2000)
3. C.H Wu, D. Wang, C.M Wang, L.J Chen, S.Y Cho, W. Staud, N. Schumann, C. Wu, "High Transmission PSM Inspection Sensitivity" Proc. SPIE BACUS, Sept 1999
4. J. Novak et al: "Defect Disposition Using Mask Printability on Attenuated Phase Shift Production Photomasks", *SPIE Proceedings of Photmask Japan* (2001)

7 ACKNOWLEDGMENTS

The authors would like to thank Emanuele Baracchi and Ernesto Villa of STMicroelectronics for their helpful contribution to this paper. We also would like to thank Simon Kurin and Shirley Hemar for their applications support.

Trademarks:
Etec is a registered trademark and ARIS is a trademark of Etec Systems, Inc., an Applied Materials company. All other trademarks are the property of their respective owners.